Available online at www.sciencedirect.com

SCIENCE DIRECT®

Journal of Catalysis 233 (2005) 434–441

JOURNAL OF CATALYSIS

www.elsevier.com/locate/jcat

Activation of O_2 and CH_4 on yttrium-stabilized zirconia for the partial oxidation of methane to synthesis gas

Jianjun Zhu [a], Jan G. van Ommen [a], Henny J.M. Bouwmeester [b], Leon Lefferts [a,*]

[a] *Catalytic Processes and Materials, Faculty of Science & Technology, Institute of Mechanics, Processes and Control Twente (IMPACT), University of Twente, PO Box 217, 7500 AE Enschede, The Netherlands*

[b] *Inorganic Materials Science, Faculty of Science & Technology, MESA$^+$ Research Institute for Nanotechnology, University of Twente, PO Box 217, 7500 AE, Enschede, The Netherlands*

Received 3 March 2005; revised 11 May 2005; accepted 13 May 2005

Abstract

The isotopic exchange reaction on ZrO_2 and yttrium-stabilized ZrO_2 (YSZ) during catalytic partial oxidation of methane to synthesis gas (CPOM) was studied with transient pulse experiments. The results reveal, surprisingly, that CPOM over both oxides proceeds via a Mars–van Krevelen mechanism. Despite the presence of adsorbed oxygen species, as confirmed by isotopic exchange experiments under reaction conditions, methane is selectively oxidized by lattice oxygen ions on the surfaces of YSZ and ZrO_2. At 900 °C, about 8 and 14% of lattice oxygen in the outermost surface layer of ZrO_2 and YSZ, respectively, can be extracted by methane. Extraction of lattice oxygen results in the formation of surface oxygen vacancies. However, the routes for replenishing oxygen differ for the two oxides. For ZrO_2, the extracted lattice oxygen ions are replenished by direct activation of molecular oxygen at the site of the surface vacancy. The presence of a high concentration of surface oxygen vacancies on YSZ, generated by doping of ZrO_2 with Y_2O_3, permits fast activation of oxygen molecules and fast lattice diffusion of oxygen. The two effects together lead to a rapid replenishment of the surface lattice oxygen extracted by methane. The proposed mechanism explains both the comparatively high activity of YSZ in CPOM and the observation that, in contrast to ZrO_2, lattice oxygen is found exclusively in oxidation products of methane over YSZ during pulse experiments.

Keywords: Catalysis; Zirconia; Yttrium-stabilized zirconia; Selective oxidation; Reaction mechanism; Oxygen vacancies; Partial oxidation of methane; Isotopic oxygen exchange

1. Introduction

The use of natural gas as a raw material is a future goal of strategic importance, because of the impending decline in fossil-oil resources and, contemporarily, the large amounts of natural gas found worldwide. The processes for the direct production of olefins and oxygenates, such as methanol and formaldehyde, are not attractive because of the low yields obtained. Therefore, considerable academic and industrial research has been focused on indirect processes proceeding via synthesis gas. Compared with steam reforming of methane, the conventional process for synthesis gas production, partial oxidation of methane to synthesis gas (POM), is attractive because of its mild exothermic heat of reaction and the suitable H_2/CO ratio for downstream processes, such as methanol and Fischer–Tropsch syntheses. Unlike noncatalytic partial oxidation, which needs a high temperature (>1200 °C) to ensure complete conversion of CH_4 and to reduce soot formation, catalytic partial oxidation (CPOM) would significantly decrease the reaction temperature with the use of active catalysts. This makes CPOM an interesting proposition for synthesis gas production.

Normally, CPOM is carried out at a still relatively high temperature (above 900 °C). The volatility of support ma-

---

[*] Corresponding author. Fax: +31-53-4894683.
E-mail address: l.lefferts@tnw.utwente.nl (L. Lefferts).

0021-9517/$ – see front matter © 2005 Elsevier Inc. All rights reserved.
doi:10.1016/j.jcat.2005.05.012

terials or of the active catalytic components is usually not considered a problem. However, in the case of catalytic oxidation at these high temperatures, volatilization of the active phase must be considered an important factor for deactivation of the catalyst. As we discussed in our previous work [1–3], metallic catalysts undergo deactivation due to sintering and metal loss via evaporation in the form of volatile metal oxides [4]. The stability of metal catalysts is still a concern, despite the fact that CPOM over metallic catalysts has been intensively studied for about two decades [5–7]. Some hardly reducible oxides, possessing very good thermal stability, have been investigated for partial oxidation of methane to synthesis gas [1–3,8–10]. Yttrium-stabilized zirconia (YSZ) appeared to be a promising catalyst for CPOM, despite its insufficient reforming activity, which needs to be compensated for with a reforming catalyst in a dual-bed system, as proposed in our previous work [1].

In general, it is known that defects, such as oxygen vacancies, are important in the surface chemistry and catalysis of metal oxides [11]. The number of oxygen vacancies in ZrO_2 can be increased significantly by doping with lower valence metal ions, such as Y^{3+} and Ca^{2+}. Compared with ZrO_2, the improved catalytic performance of YSZ in oxidation catalysis has been attributed to a high concentration of oxygen vacancies [3,12]. Lattice oxygen ions are often involved in reactions over oxide catalysts. Most of the partial oxidation reactions proceed via a Mars–van Krevelen mechanism, in which lattice oxygen ions are incorporated into the products [13]. The cycle for catalytic partial oxidation is closed via replenishment of the extracted lattice oxygen ions through the dissociative adsorption of molecular oxygen at the surface [14].

In our previous work [2], formaldehyde and formate were both shown to be reaction intermediates for CPOM over YSZ. Based on the results of in situ FTIR and both steady-state and transient experiments, a reaction scheme was proposed. We also investigated the effect of the surface composition of YSZ catalysts on the catalytic performance in CPOM. It was postulated that oxygen vacancies are most likely involved in CPOM [3]. However, the mechanistic details, particularly the role of oxygen vacancies and that of lattice oxygen ions in the partial oxidation of methane, are still not clear. Moreover, the nature of the oxygen species, such as surface lattice oxygen ions or adsorbed oxygen, in the activation of methane is still a matter of controversy [15,16].

In this work we identify the active sites for the activation of both oxygen and methane on the surfaces of YSZ and ZrO_2. CPOM is studied over ZrO_2-based catalysts in transient experiments. Isotopic oxygen $^{18}O_2$ exchange with the catalysts is investigated in both the absence and presence of methane and under reaction conditions for CPOM.

2. Experimental

2.1. Catalysts

We prepared catalyst samples of ZrO_2 and YSZ by calcining powders of pure zirconia and stabilized zirconia with 14 wt% Y_2O_3, respectively, at 900 °C. The YSZ sample used in this study is identical to the catalyst YSZ14A described in our previous work [3]. After calcination for 15 h in air, the BET surface areas were 13.7 and 15.4 m^2/g for YSZ and ZrO_2, respectively. TiO_2 and HfO_2 were found to be two major contaminations in the bulk, whereas no inorganic contamination was detected on the outermost layer by low-energy ion scattering (LEIS). More details about catalyst preparation and characterization are presented in our previous work [3].

2.2. Transient experiments

Pulse experiments using CH_4 and/or O_2 were performed in an alumina reactor with an inner diameter of 4 mm. Helium (40 ml/min) with a purity of 99.99% was used as a carrier gas. The effluent from the reactor was analyzed by an on-line quadrupole mass spectrometry (Balzers QMS 200F). Significant contributions of gas-phase reactions and/or α-Al_2O_3 (diluent of the catalyst bed) were not observed in blank experiments with an empty reactor and/or α-Al_2O_3 instead of the catalyst. The pulse experimental data were used primarily to determine the amount of oxygen that was removed from or reintroduced into the catalyst during each reduction and oxidation cycle. We calibrated the mass spectrometer by pulsing different amounts of reactants or products of CPOM through the α-Al_2O_3 bed. The amount of each compound was estimated based on the area of the corresponding peak (m/e intensity with time). Before pulsing, the catalyst (0.3 g diluted with 0.3 g α-Al_2O_3) was pre-oxidized in a mixture of O_2 (40 ml/min) and He (40 ml/min) at 800 °C for 1 h. Subsequently, the reaction system was cooled or heated to the reaction temperature and flushed with helium (40 ml/min) for 1 h to remove any residual oxygen in the system. Then a sequence of pulses of methane (500 µl per pulse) was passed through the catalyst bed with an interval time of 5 min. After oxygen was exhausted from the catalyst by reaction with subsequent pulses of methane, the system was flushed with helium for 0.5 h to remove possible residual CH_4. We studied the re-oxidation of the catalyst by pulsing with pure O_2 (99.99%) with the same sample loop of 500 µl.

2.3. Isotopic $^{18}O_2$ exchange

Isotopic oxygen exchange between $^{18}O_2$ and the catalysts was investigated in the temperature range from 30 to 900 °C. The purity of the stable isotopic $^{18}O_2$ was not lower than 95 at% (Chemotrade, Germany). Quartz wool plugs were used to support and secure the 0.3-g catalyst sample in the middle of the alumina reactor. The outlet gas was analyzed by on-line mass spectrometry (Balzers QMS 200F). The oxygen balance in the experiments was 98 ± 2%. Before pulsing with $^{18}O_2$, the sample was pre-oxidized with 80 ml/min of O_2/He (1/1) at 800 °C for 1 h to remove adsorbed contaminations, such as H_2O and CO_2. Subsequently, the system was cooled or heated to the temperature for the oxygen exchange experiment and flushed with He (80 ml/min) at the same temperature for 1 h. After this pretreatment, a pulse of $^{18}O_2$ was passed through the catalyst bed with 40 ml helium/min as carrier gas. Before the exchange experiment was carried out at another temperature, the catalyst was re-oxidized with O_2/He and flushed with helium again as described above. The pulse size was equivalent to 2.7×10^{19} oxygen atoms (500-µl loop) or 1.35×10^{18} oxygen atoms (25-µl loop). We studied the influence of methane on the oxygen exchange reaction by simultaneously pulsing CH_4 (50 µl) and $^{18}O_2$ (25 µl) into the carrier gas via two six-port valves, resulting in one $^{18}O_2$–CH_4 pulse.

3. Results

3.1. Isotopic oxygen exchange

3.1.1. $^{18}O_2$ exchange in the absence of methane

$^{18}O_2$ exchange experiments were conducted at temperatures between 30 and 900 °C over ZrO_2 and YSZ. These two catalysts had almost identical surface areas (14.5 ± 1.0 m^2/g). All possible oxygen molecules ($^{18}O_2$, $^{16}O\,^{18}O$, and $^{16}O_2$) were monitored at the reactor outlet. Blank experiments showed that the $^{18}O_2$ conversion was less than 5% in the empty alumina reactor, even at 900 °C. The product distribution for the $^{18}O_2$ exchange with YSZ and ZrO_2 as a function of reaction temperature is shown in Fig. 1. Note that each data point represents a single isothermal experiment and that the pulse amount is about equivalent to the amount of oxygen in one monolayer. Very small amounts of $^{16}O\,^{18}O$ and $^{16}O_2$ were detected at temperatures below 300 °C, which originate from impurities in the $^{18}O_2$ gas. Oxygen exchange occurs at temperatures above 300 °C for both ZrO_2 and YSZ. Both $^{16}O_2$ and $^{16}O\,^{18}O$ were observed as isotopic exchange products when $^{18}O_2$ was pulsed over the catalysts. Unlike for $^{16}O_2$, showing a steadily increasing concentration with reaction temperature, a maximum in the amount of $^{16}O\,^{18}O$ was observed at 625 °C for ZrO_2 and at 575 °C for YSZ. $^{16}O\,^{18}O$ was the major isotopic product at temperatures below 575 °C for YSZ, whereas the presence of $^{16}O_2$ increased significantly at the expense of $^{16}O\,^{18}O$ at temperatures above 575 °C. Only $^{16}O_2$ was detected at temperatures above 800 °C for both ZrO_2 and YSZ. Even after ten $^{18}O_2$ pulses with a loop of 500 µl, $^{16}O_2$ was detected exclusively.

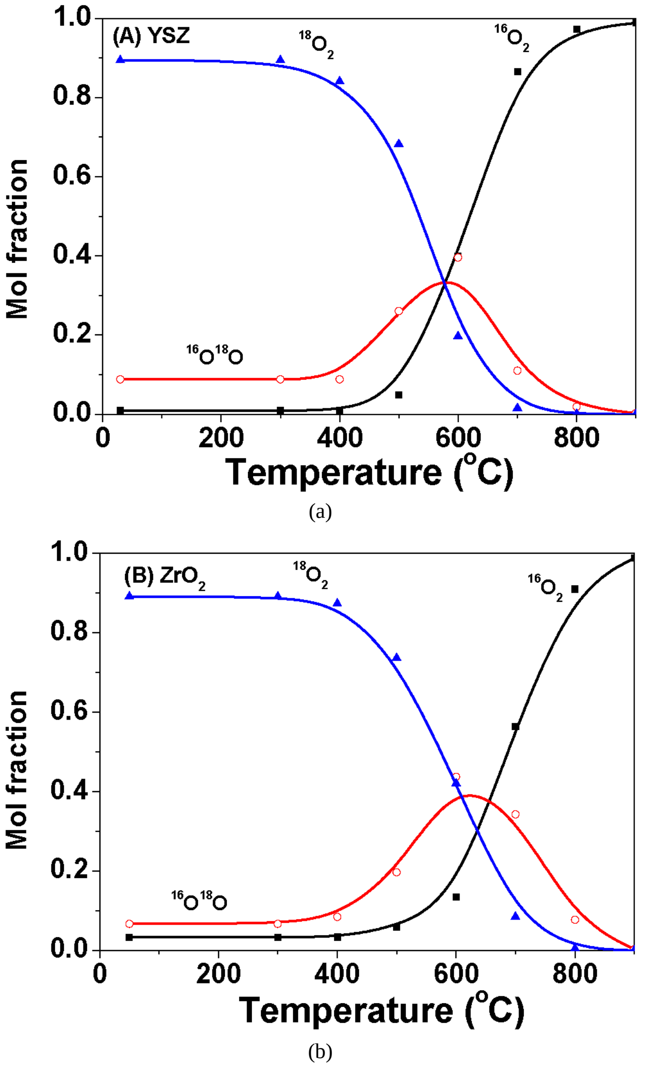

(a)

(b)

Fig. 1. Dependence of isotopic product distribution on reaction temperature when pulsing $^{18}O_2$ (1.34×10^{19} molecules/pulse) over (a) 0.3 YSZ ($S_g = 13.7\ m^2/g$), and (b) 0.3 g ZrO_2 ($S_g = 15.4\ m^2/g$).

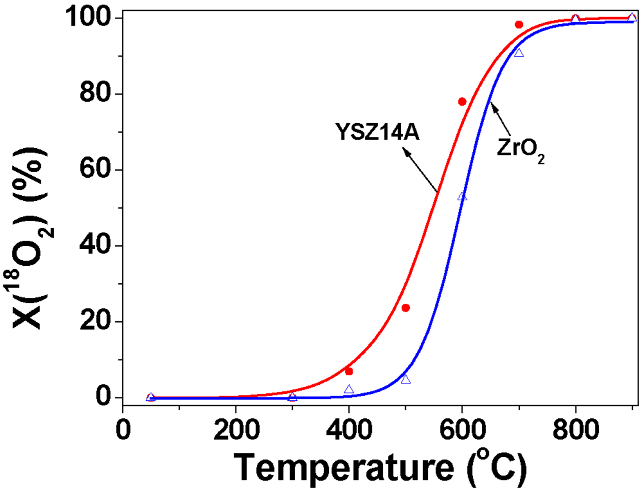

Fig. 2. Temperature dependence of the conversion of gas-phase $^{18}O_2$ (2.68×10^{19} atoms/pulse) in the isotopic exchange reaction with ZrO_2 and YSZ.

The temperature dependence of the conversion of $^{18}O_2$ during the exchange with ZrO_2 and YSZ is shown in Fig. 2. At temperatures below 700 °C, the oxygen exchange reaction was found to be significantly slower for ZrO_2, compared with that of YSZ. Complete exchange is observed for both ZrO_2 and YSZ at temperatures above 800 °C.

3.1.2. $^{18}O_2$ exchange in the presence of methane

We investigated the influence of methane on the oxygen exchange reaction by pulsing CH_4 (50 µl/pulse) and $^{18}O_2$ (25 µl/pulse) simultaneously over 0.3 g YSZ or ZrO_2. All possible products (H_2, $H_2{}^{16}O$, $H_2{}^{18}O$, $C^{16}O$, $C^{18}O$, $C^{16}O_2$, $C^{16}O^{18}O$, $C^{18}O_2$) were monitored by mass spectrometry at the outlet of the reactor. The product responses of the $^{18}O_2$–CH_4 pulse over YSZ and ZrO_2 at 600 °C are shown in Figs. 3a and b. Surprisingly, the products detected for YSZ (Fig. 3a) were limited to $C^{16}O$, $C^{16}O_2$, $H_2{}^{16}O$, and H_2, whereas no products containing ^{18}O could be detected. Similar results were obtained at 800 °C. Obviously, these products were formed via oxidation of methane with ^{16}O originating from YSZ. Compared with pulsing of CH_4 exclusively, as described in Section 3, all product responses increased significantly when CH_4 was pulsed together with $^{18}O_2$. Unlike for YSZ, a significant amount of $C^{16}O^{18}O$ was detected when for pulsing of $^{18}O_2$–CH_4 over ZrO_2, although ^{16}O-containing products were again found to be dominant (Fig. 3b). Fig. 4 compares the oxygen responses for $^{18}O_2$ and $^{18}O_2$–CH_4 pulses over YSZ at 600 °C. The presence of methane induces a strong decrease in the amounts of $^{16}O_2$ and $^{16}O\,^{18}O$ detected, whereas the amount of $^{18}O_2$ decreases only slightly.

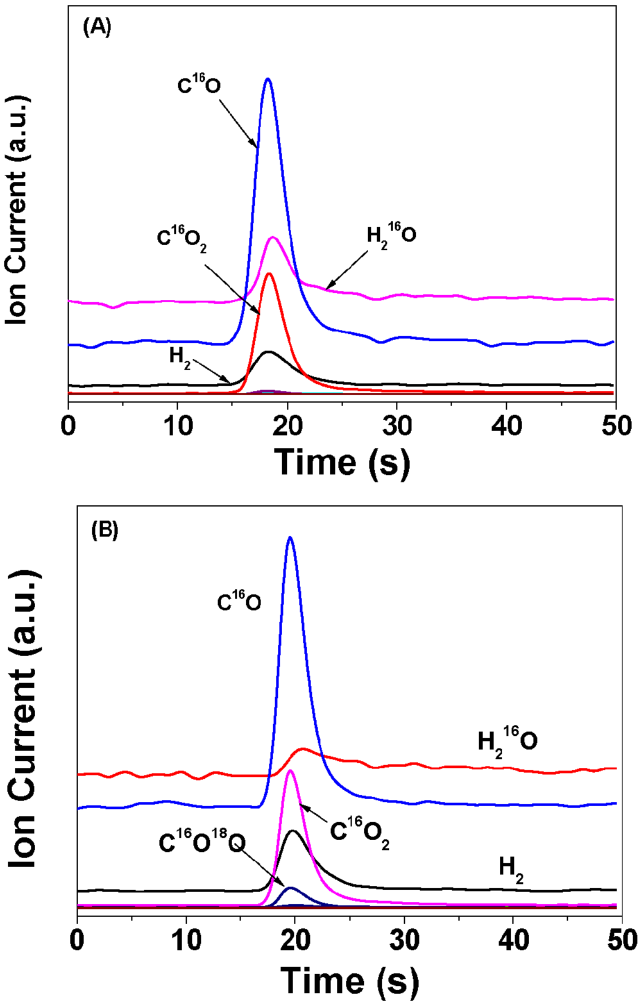

Fig. 3. Product response of $^{18}O_2$–CH_4 pulse (25 µl $^{18}O_2$ plus 50 µl CH_4) over (a) 0.3 g YSZ and (b) 0.3 g ZrO_2 at 600 °C.

3.2. Methane activation

3.2.1. CH_4-pulse experiments

CH_4 pulse experiments over both ZrO_2 and YSZ were carried out in the absence of oxygen at 900 °C and 1 bar. Possible traces of oxygen in the carrier gas (helium) were not significant, because variation of the time interval between CH_4 pulses did not influence the experimental results. The product responses of a CH_4 pulse over pre-oxidized YSZ are shown in Fig. 5. A mixture of CO, H_2, CO_2, and

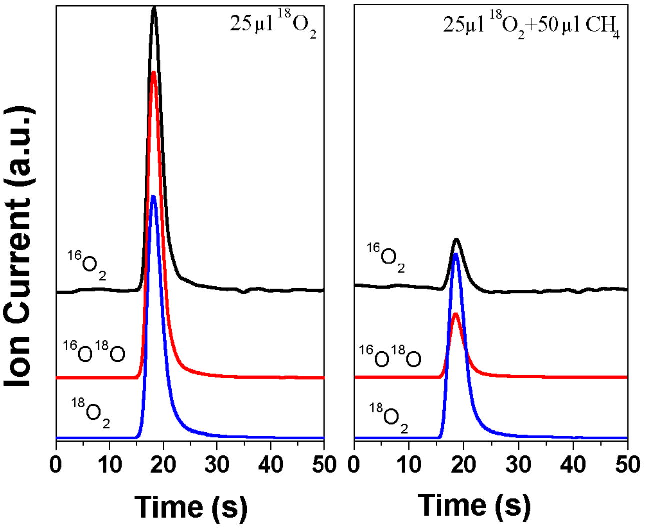

Fig. 4. Oxygen response during $^{18}O_2$ pulse and $^{18}O_2$–CH_4 pulse over 0.3 g YSZ at 600 °C.

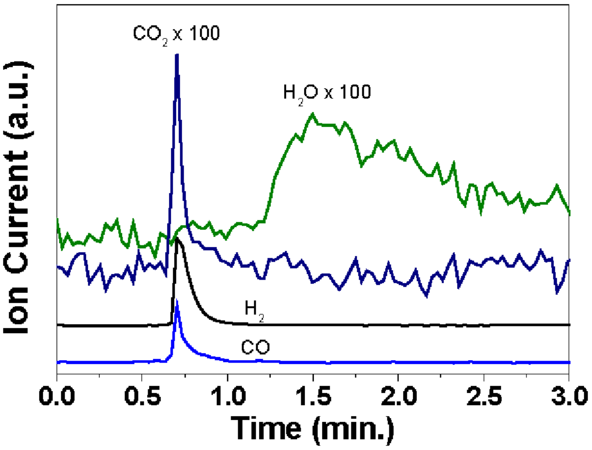

Fig. 5. Response of a methane pulse over 0.3 g YSZ at 900 °C. The catalyst was pre-oxidized for 1 h, followed by flush with helium for 1 h, both at 800 °C.

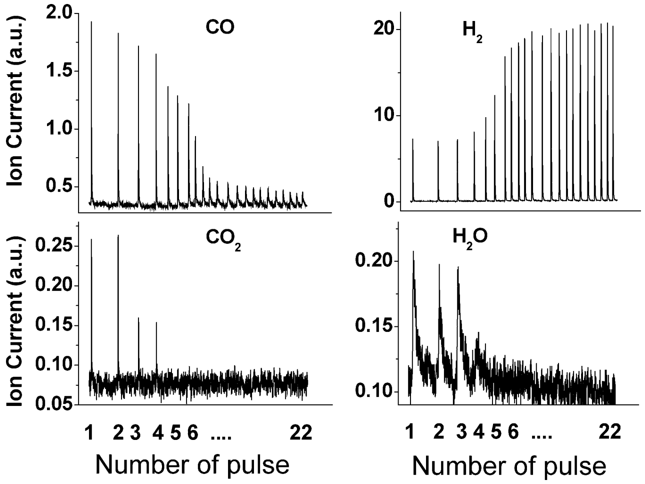

Fig. 6. Effluent gases from methane pulsing experiment at 900 °C over 0.3 g YSZ ($S_g = 13.7\ m^2/g$), which was pre-oxidized at 900 °C for 1 h and subsequently flushed with helium for 1 h.

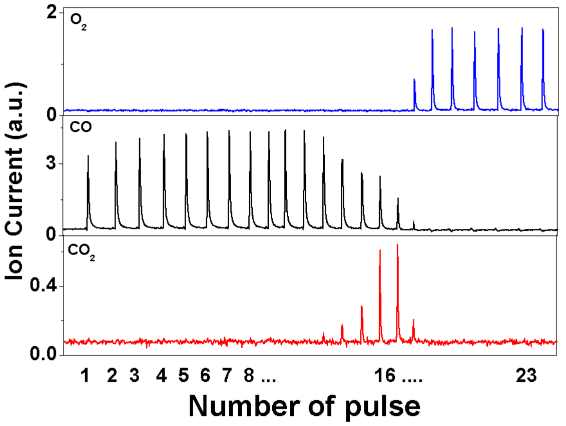

Fig. 7. Effluent gases from O_2 (50 µl/pulse) pulsing experiment at 900 °C over 0.3 g YSZ ($S_g = 13.7\ m^2/g$) after 22 methane pulses.

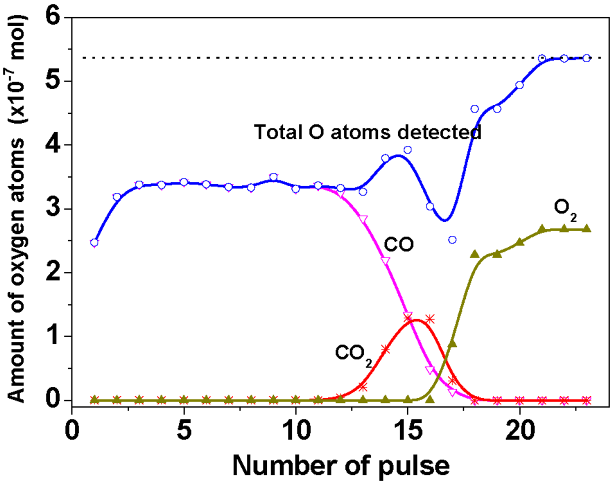

Fig. 8. Amounts of oxygen atom contained in the effluent gases of each oxygen pulse over 0.3 g YSZ after 22 methane pulses.

H_2O was produced during the pulse experiments, which is in agreement with the product mixture in steady-state experiments [2]. Unlike other products, a delayed signal is observed for H_2O, suggesting a strong adsorption of H_2O on YSZ catalysts. The formation of CO, CO_2, and H_2O may result from CH_4 reacting with active oxygen species on/in YSZ. The product distribution versus pulse number is shown in Fig. 6. CO_2 and H_2O were formed only during the first four pulses, whereas CO and H_2 were formed during all methane pulses. The concentration of active oxygen species on/in YSZ was apparently too low to deeply oxidize CH_4 after four pulses. After about 10–13 pulses, very small but constant signals for m/e of 28 were observed. These can be attributed to a trace of N_2 (about 20 ppm) in the CH_4 gas, which has the same mass-to-charge ratio ($m/e = 28$) as CO. Upon further pulsing, dissociation of CH_4 resulted in a higher H_2 signal, and carbon deposition occurred on the YSZ surface after oxygen was exhausted from the catalyst. Similar results were obtained for ZrO_2.

After we subtracted the contribution of the trace of nitrogen in CH_4 gas, we estimated that about $6.3 \pm 0.5 \times 10^{17}$ and $5.5 \pm 0.5 \times 10^{17}$ oxygen atoms per square meter (O/m^2) were extracted by CH_4 pulses from pre-oxidized ZrO_2 and YSZ, respectively. These values were estimated from the amounts of CO, CO_2, and H_2O formed.

Identical pulse experiments were carried out over pre-reduced YSZ and ZrO_2, which were treated with 5% H_2 in argon at 900 °C for 1 h before pulsing with CH_4. H_2 was formed by decomposition of CH_4, and no oxygen-containing products were detected.

3.2.2. O_2-pulse experiments

O_2 pulses were conducted over the catalyst at 900 °C and 1 bar, after oxygen was exhausted by 22 CH_4 pulses as described above. Before pulsing with O_2, the catalyst was flushed with pure helium at 900 °C for 30 min. The responses of oxidation products and oxygen during oxygen pulses over YSZ are shown in Fig. 7. CO and CO_2 were the two oxidation products observed during pulsing with oxygen; that is, H_2 and H_2O were not detected. During the first 12 pulses, only CO was formed. An increasing CO_2 signal was observed starting from the 13th pulse at the expense of CO. Oxygen was first detected at the 17th pulse, where very small amounts of CO and CO_2 were produced. Constant oxygen signals were observed after 18 pulses, and no products were detected.

The amount of oxygen atoms in the effluent gas after each pulse is shown in Fig. 8. In this figure, the dotted line displays the amount that was contained in each single oxygen pulse. Obviously, the total amount of oxygen atoms in O_2, CO, and CO_2 detected in the effluent was less than the oxygen pulsed for the first 21 pulses. The missing oxygen was apparently stored in the oxide catalyst via re-oxidation of the catalyst. The integral amounts of oxygen stored in YSZ and ZrO_2 were about $6.1 \pm 0.5 \times 10^{17}\ O/m^2$ and $10.3 \pm 1.0 \times 10^{17}\ O/m^2$, respectively.

4. Discussion

4.1. Oxygen activation

Fig. 1 clearly shows $^{18}O_2$ isotopic exchange with ZrO_2 and YSZ at temperatures above 300 °C. Each pulse contained 2.7×10^{19} ^{18}O atoms, which is approximately equivalent to the number of oxygen ions in one monolayer of 0.3 g ZrO_2 or YSZ, each of which had a total surface area of 4.5 m^2. At temperatures above 800 °C, $^{18}O_2$ was completely exchanged with ^{16}O originating from ZrO_2 or YSZ, even after ten pulses.

It has been recognized that anionic defects, such as oxygen vacancies and F centers (an oxygen vacancy capturing one or two electrons), favor the oxygen exchange reaction [17–21]. This would explain the observation in Fig. 2 that oxygen exchange is much slower on ZrO_2 than on YSZ. The latter has a much higher concentration of oxygen vacancies generated by doping of Y_2O_3 in ZrO_2.

Isotopic oxygen exchange has been studied on many oxides, including YSZ [22–24], and several strongly similar mechanisms have been proposed. According to the generally adopted kinetic scheme [25,26],

$$O_2 + e' \Longleftrightarrow O_2^-, \qquad O_2{}^- + e' \Longleftrightarrow O_2{}^{2-},$$

$$O_2{}^{2-} \Longleftrightarrow 2O^- \qquad \text{dissociation;}$$

$$O^- + V_{o,s}^{\cdot\cdot} + e' \Longleftrightarrow O_{o,s}^{\times} \qquad \text{incorporation;}$$

$$O_{o,s}^{\times} + V_{o,b}^{\cdot\cdot} \Longleftrightarrow O_{o,b}^{\times} + V_{o,s}^{\cdot\cdot} \qquad \text{diffusion;}$$

several species can occur as intermediates for the reduction of molecular oxygen, such as $O_2{}^-$, $O_2{}^{2-}$, and O^-. In this work we do not attempt to distinguish between these three surface oxygen species, and therefore they are denoted as O^* hereafter. The Kröger-Vink notation is used for lattice defects: $V_o^{\cdot\cdot}$ denotes an oxygen vacancy, $O_o^{\times}$ a regular lattice oxygen ion, and e' an electron. The footnotes s and b refer to "surface" and "bulk," respectively. Thereby we make a distinction between lattice oxygen ions fully coordinated in the bulk versus lattice oxygen ions in the surface, which are necessarily not coordinatively saturated. This distinction is necessary because only the surface lattice oxygen will be accessible for the catalytic reaction. The same argument also holds for oxygen vacancies. In principle, each of the indicated reaction steps may be rate determining.

The distribution of isotopic exchange products depends on the relative rates of the dissociation, incorporation, and diffusion steps. Note that the randomization of isotopic components can occur only after dissociation of the oxygen molecule at the surface. Hence, if the incorporation reaction and subsequent diffusion are faster, $^{16}O_2$ will be the dominating product. In contrast, faster dissociation of oxygen compared with oxygen incorporation will lead to formation of $^{16}O\,^{18}O$. Fig. 1 shows that more $^{16}O\,^{18}O$ is formed than $^{16}O_2$ at temperatures below 575 °C for YSZ and 625 °C for ZrO_2. This shows that the dissociation of oxygen is relatively fast at these temperatures. This observation is in good agreement with results obtained by Manning et al. [23,24], who reported that incorporation of oxygen species with YSZ is rate determining below 700 °C, whereas dissociation is rate determining above this temperature.

4.2. Methane activation

Surprisingly, Fig. 3a shows exclusive formation of ^{16}O-containing products during CH_4–$^{18}O_2$ pulsing experiments. This is, first of all, strong evidence for the participation of oxygen originating from YSZ in the catalytic oxidation of methane. Furthermore, the fact that no ^{18}O-containing products are detected excludes the possibility of methane oxidation in the gas phase at temperatures up to 800 °C. The formation of $^{16}O_2$ and $^{16}O\,^{18}O$ in Fig. 4 confirms the existence of both $^{16}O^*$ and $^{18}O^*$ on the surface of YSZ during the CH_4–$^{18}O_2$ pulse. In essence, this is consistent with the data from oxygen exchange experiments shown in Fig. 1. The formed amounts of $^{16}O_2$ and $^{16}O\,^{18}O$ in Fig. 4 are about similar, indicating comparable surface concentrations of $^{16}O^*$ and $^{18}O^*$ at 600 °C. The combined observations made in Figs. 3a and 4 thus lead to the conclusion that the type of oxygen that reacts with methane is lattice oxygen ion ($O_{O,\,s}^{\times}$) in the outermost surface layer of YSZ, as opposed to adsorbed surface oxygen (O^*) that is also present. The data also imply that no accumulation of $^{18}O_{O,\,s}^{\times}$ occurs in the outermost surface layer during the CH_4–$^{18}O_2$ pulse, which in turn suggests that incorporation of oxygen and subsequent diffusion into the bulk and vice versa are comparatively fast as compared with methane activation. A similar conclusion was drawn from data from isotopic exchange experiments carried out by Ishihara et al. [21].

Finally, Fig. 4 shows that the oxidation of CH_4 competes in a way with isotopic oxygen exchange. In spite of a slightly enhanced $^{18}O_2$ conversion in the presence of CH_4 (cf. $^{18}O_2$ signals in Figs. 4a and b), the consumption of lattice oxygen ions ($^{16}O_{O,\,s}^{\times}$) by methane suppresses the formation of $^{16}O^*$ at the surface, which is why the formation rates of $^{16}O_2$ and $^{16}O\,^{18}O$ decrease significantly. The enhanced conversion of $^{18}O_2$ in the presence of CH_4 suggests that CH_4 and O_2 molecules at the surface are *not* competing for the same adsorption sites, in agreement with a redox mechanism.

Figs. 5 and 6 demonstrate that methane was preferentially oxidized by lattice oxygen when YSZ or ZrO_2 was pre-oxidized. No oxidation products were observed when CH_4 was pulsed over pre-reduced YSZ or ZrO_2 at 900 °C (not shown). It should be noted that the amount of removable oxygen in both ZrO_2 and YSZ was found to be below the detection limit of conventional TPR. Partial reduction of ZrO_2 has been reported by other researchers [27,28], although ZrO_2 and YSZ are normally considered to be irreducible oxides. Re-oxidation of oxygen-exhausted YSZ and ZrO_2 confirms that CPOM over both YSZ and ZrO_2 proceeds via a Mars–van Krevelen mechanism [29]. Corresponding data are shown in Figs. 6 and 8. Compared with the amount of oxygen replenished ($6.1 \pm 0.5 \times 10^{17}$ O/m^2 and $10.3 \pm 1.0 \times 10^{17}$ O/m^2 for YSZ and ZrO_2, respectively) (Fig. 8), the amount of oxygen extracted by pulses of CH_4 (Fig. 6) was lower ($5.5 \pm 0.5 \times 10^{17}$ O/m^2 and $6.3 \pm 0.5 \times 10^{17}$ O/m^2 for YSZ and ZrO_2, respectively). First of all, these numbers are of the same order of magnitude, although the difference for ZrO_2 is significant. The reason for this is the fact that quantitative analysis of water with MS is unreliable in general because of adsorption of water on the equipment and the unavoidable presence of water in the background of the vacuum. Moreover, it was not possible to calibrate the MS for water in the correct low-concentration range. The experiments with ZrO_2 were more affected than those with YSZ because the amount of water produced on ZrO_2 was significantly larger. Nevertheless, in the O_2 pulse experiments no water was formed, therefore providing the most reliable numbers for the amount of oxygen that could be removed: 6.1×10^{17} O/m^2 and 10.3×10^{17} O/m^2 for YSZ and ZrO_2, respectively. If it is assumed that solely the (100) faces of monoclinic ZrO_2 and cubic YSZ are exposed to the CH_4 gas, the integral amounts of extracted lattice oxygen correspond to only 13.6 and 8.5%, respectively, of a single monolayer. Analysis with LEIS and XRF excludes significant contributions from reducible metal oxide contaminations. The amount of oxygen that can be released from ZrO_2 and YSZ bulk because of the change in oxygen activity that occurs with CH_4 pulsing was estimated based on data from the literature [30,31]. It is at least two orders of magnitude smaller than the amount extracted by CH_4 pulses. Thus, the partial reduction must be confined to the surface of the catalysts.

Fig. 6 shows the formation of CO_2, CO, H_2, and H_2O during pulsing of CH_4 over the pre-oxidized catalyst. These are all primary products of CPOM [2]. Deep oxidation of methane to CO_2 and H_2O occurs during the first four pulses, whereas partial oxidation to CO and H_2 is found to dominate during the subsequent pulses. This shows that the amount of extractable lattice oxygen of the catalyst has a significant influence on the relative rates of reactions, which is in accordance with a kinetic model presented elsewhere [2]. A low concentration of extractable lattice oxygen favors selective oxidation of methane to CO and H_2, produced mainly via decomposition of adsorbed formaldehyde. In contrast, a high concentration of extractable lattice oxygen promotes further oxidation of surface formaldehyde to CO_2 and H_2O via surface formate and carbonate intermediates.

4.3. *Reaction model*

The role of lattice oxygen in heterogeneous catalytic reactions has been the subject of many studies [13,32–35]. It has been shown that conventional redox catalysts can act as the source of active oxygen and sustain oxidation for a certain period of time in the absence of oxygen in the gas phase [33–35]. Our results show that this also holds for ZrO_2 and YSZ.

In pure ZrO_2, the intrinsic concentration of oxygen vacancies is low [36,37]. Doping with Y_2O_3 leads to formation of extrinsic oxygen vacancies. On the other hand, oxygen vacancies on the surfaces of ZrO_2 and YSZ are created by extraction of lattice oxygen ions, as revealed by characterization of adsorbed CO by in situ FTIR [38] or directly illustrated by EPR spectroscopy [12,39]. This is possible if the valence state of the catalyst rapidly adjusts itself to the external conditions. In a localized description, this leads to the formation of two Zr^{3+} surface cations associated with a single vacancy. In Kröger-Vink notation, the formed associate can be presented as $Zr'_{Zr}\text{–}\ V^{\cdot\cdot}_{O,s}\text{–}Zr'_{Zr}$. These vacancies can be re-filled with oxygen, either by direct activation of oxygen from the gas phase or by lattice oxygen diffusion. The reversed view is that surface lattice oxygen coordinated by Zr^{4+} cations is active in the methane oxidation reaction.

Although doping ZrO_2 with Y_2O_3 increases the concentration of extrinsic oxygen vacancies, it also decreases the concentration of surface lattice oxygen ($O^{\times}_{O,s}$) because the Y_2O_3 concentration in the surface is significant [3]. This explains why significantly more oxygen could be removed by subsequent methane pulses from pre-oxidized ZrO_2 than from pre-oxidized YSZ (see Section 4.2). The extent of reduction is about 13.6 and 8.5% of the total number of oxygen atoms in a single monolayer for ZrO_2 and YSZ, respectively.

Surface lattice oxygen ions are extracted during reaction with methane. In the case of ZrO_2, re-oxidation of the vacant sites by O_2 is the main route for replenishing the surface lattice oxygen. Fig. 3b shows formation of $C\,^{16}O\,^{18}O$ during a $^{18}O_2$–CH_4 pulse over ZrO_2, which is taken as evidence that the extracted oxygen on the surface of ZrO_2 is regenerated by direct activation of molecular oxygen at the surface oxygen vacancy site. In the case of YSZ, fast oxygen exchange and fast lattice oxygen diffusion provide an alternative pathway for replenishment of the surface lattice oxygen. The presence of extrinsic oxygen vacancies promotes the surface exchange reaction, but also facilitates rapid diffusion of oxygen in the lattice. This explains the higher conversion rate of methane over YSZ (8.4×10^{18} mol m^{-2} s^{-1} at 600 °C) compared with ZrO_2 (4.3×10^{18} mol m^{-2} s^{-1}) at the same temperature [3]. It also explains why ^{16}O-containing products are exclusively produced during $^{18}O_2$–CH_4 pulses over YSZ (see Fig. 3a).

The emerging picture, as depicted in Fig. 9, is that CPOM over both YSZ and ZrO_2 proceeds via the Mars–van Krevelen reduction-oxidation mechanism. For ZrO_2, the rate of methane oxidation is balanced by the rate of re-oxidation of the vacant sites by O_2. In the case of YSZ, fast diffusion of oxygen in conjunction with rapid oxygen activation at extrinsic oxygen vacancies at the surface provides an alternative pathway for replenishment of the oxygen consumed by methane. The significant difference in the catalytic performance of ZrO_2 and YSZ, as also reported in our early work [3], is due to the difference in the defect chemistry of these two catalysts, which is related to the generation of the extrinsic oxygen vacancies $Y'_{Zr}\text{–}\ V^{\cdot\cdot}_{O,\,s}\text{–}Y'_{Zr}$. The present re-

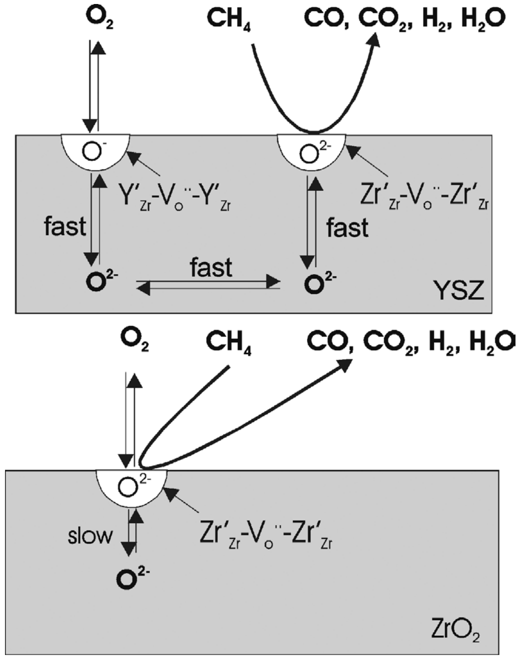

Fig. 9. The reaction models proposed for CPOM over YSZ and ZrO_2 catalysts.

sults make it apparent that it is the activation of methane on the YSZ surface, rather than the activation of molecular oxygen, that is the rate-determining step during CPOM (see Fig. 4b).

5. Conclusions

The results of this study clearly demonstrate that CPOM over ZrO_2 and YSZ proceeds via a Mars–van Krevelen mechanism. Methane is selectively oxidized by surface lattice oxygen. At 900 °C, about 8 and 14% of lattice oxygen in the outermost surface layer of ZrO_2 and YSZ, respectively, can be extracted by methane. Extraction of lattice oxygen by methane results in the formation of surface oxygen vacancies. After this oxidation step, the route for replenishing surface oxygen differs for the two oxides. For ZrO_2, the replenishment occurs by direct activation of molecular oxygen at the surface oxygen vacancy site. Extrinsic oxygen vacancies in YSZ, generated by doping ZrO_2 with Y_2O_3, facilitate fast activation of molecular oxygen and fast lattice diffusion of oxygen. The two effects together lead to a rapid replenishment of the surface lattice oxygen extracted by methane. The proposed mechanism explains both the comparatively high activity of YSZ in CPOM and the observation that, in contrast to ZrO_2, lattice oxygen is found exclusively in oxidation products of methane over YSZ during the pulse experiments.

Acknowledgments

This work was performed under the auspices of NIOK, the Netherlands Institute of Catalysis Research. Stichting Technische Wetenschappen (STW, the Dutch technology foundation) is gratefully acknowledged for financial support under project number UPC-5037. The authors thank Mr. Sander Albertsma for part of the CH_4 pulse experiments and Ing. Bert Geerdink for technical support.

References

[1] J. Zhu, M.S.M.M. Rahuman, J.G. van Ommen, L. Lefferts, Appl. Catal. A 259 (2004) 95.
[2] J. Zhu, J.G. van Ommen, L. Lefferts, J. Catal. 225 (2004) 388.
[3] J. Zhu, J.G. van Ommen, A. Knoester, L. Lefferts, J. Catal. 230 (2005) 300.
[4] R.A. Dalla Betta, Catal. Today 35 (1997) 129.
[5] D.A. Hickman, L.D. Schmidt, Science 259 (1993) 343.
[6] D.A. Hickman, L.D. Schmidt, AIChE J. 39 (1993) 1164.
[7] A.T. Aschcroft, P.D.F. Vernon, M.L.H. Green, Nature 344 (1990) 319.
[8] A.G. Steghuis, PhD thesis, University of Twente, The Netherlands, 1998.
[9] A.G. Steghuis, J.G. van Ommen, J.A. Lercher, Catal. Today 46 (1998) 91.
[10] E.R. Stobbe, PhD thesis, University of Utrecht, The Netherlands, 1999.
[11] M.A. Barteau, J. Vac. Soc. Technol. A 11 (1993) 2162.
[12] M. Labaki, S. Siffert, J.F. Lamonier, E.A. Zhilinskaya, A. Aboukais, Appl. Catal. B 43 (2003) 261.
[13] Z.X. Liu, Q.X. Bao, N.J. Wu, J. Catal. 113 (1988) 45.
[14] A. Belansky, J. Haber, Marcel Dekker, New York, 1996.
[15] J.H. Lunsford, Stud. Surf. Sci. Catal. 81 (1994) 1.
[16] Z. Zhang, X.E. Verykios, M. Baerns, Catal. Rev.-Sci. Eng. 36 (1994) 507.
[17] E.N. Voskresenskaya, V.G. Roguleva, A.G. Anshits, Catal. Rev.-Sci. Eng. 37 (1995) 101.
[18] E.R.S. Winter, J. Chem. Soc. A (1968) 2889.
[19] E.R.S. Winter, J. Chem. Soc. A (1969) 1832.
[20] S.Z. Lacombe, H.M. Zanthoff, C. Mirodatos, J. Catal. 155 (1996) 106.
[21] T. Ishihara, et al., Solid State Ionics 593 (1998) 113–115.
[22] N. Sakai, et al., Phys. Chem. Chem. Phys. 5 (2003) 2253.
[23] P.S. Manning, J.D. Sirman, J.A. Kilner, Solid State Ionics 93 (1997) 125.
[24] P.S. Manning, J.D. Sirman, R.A. De Souza, J.A. Kilner, Solid State Ionics 100 (1997) 1.
[25] R. Merkle, J. Marier, Phys. Chem. Chem. Phys. 4 (2002) 4140.
[26] B.A. Boukamp, B.A. van Hassel, I.C. Vinke, K.L. de Vries, A.J. Burgraaf, Electrochem. Acta 38 (1993) 1817.
[27] S.M. Stagg, E. Romeo, C. Padro, D.E. Resasco, J. Catal. 178 (1998) 137.
[28] S. Sharma, S. Hilaire, J.M. Vohs, R.J. Gorte, H.W. Jen, J. Catal. 190 (2000) 199.
[29] P. Mars, D.W. van Krevelen, Chem. Eng. Sci. 3 (1954) 41.
[30] J. Xue, R. Dieckmann, J. Electrochem. Soc. 138 (1991) 36C–40C.
[31] W. Weppner, Naturforsch 31a (1976) 1336–1343.
[32] M.E. Lashier, G.L. Schrader, J. Catal. 128 (1991) 113.
[33] T.V. Andrushkevich, Catal. Rev.-Sci. Eng. 35 (1993) 213.
[34] V.D. Sokolowsky, Catal. Rev.-Sci. Eng. 32 (1990) 1.
[35] Y. Schuurman, J.T. Gleaves, J.R. Ebner, M.J. Munney, Stud. Surf. Sci. Catal. (1994) 82.
[36] N. Mommer, T. Lee, J.A. Gardber, W.E. Evenson, Phys. Rev. B 61 (2000) 162.
[37] E. Karaoetrova, et al., J. Am. Ceram. Soc. 84 (2001) 65.
[38] C. Morterra, E. Giamello, L. Orio, M. Volante, J. Phys. Chem. 94 (1990) 3111.
[39] Q. Zhao, X. Wang, T. Cai, Appl. Surf. Sci. 225 (2004) 7.